

MOLECULAR DYNAMICS STUDY OF INFINITELY THIN HARD RODS. COMPUTER
EXPERIMENTS ON DYNAMICAL SCALING.

Daan Frenkel and John F. Maguire

Molecular Dynamics (MD) calculations are widely used to study the structural and dynamical properties of atomic and molecular fluids. Often, such calculations provide the only tool to test predictions of statistical-mechanical theories of transport phenomena in dense fluids on a microscopic scale. Many of the recent developments in liquid state theory have been inspired by the results of computer simulations (see e.g. ref.1). Among the systems studied, the hard-sphere system has played a special role^{2,3}. The reason is twofold: computer simulations on the hard-sphere system could be used to test existing theories of the liquid state such as the Percus-Yevick equation (equilibrium properties) and the Enskog expressions for transport properties. Such tests, and the discrepancies they revealed (e.g. Alders test of the Enskog theory of molecular diffusion) form the starting point for many of the modern theories of dense fluids. A second reason why the hard-sphere system has played a special role is that, once its properties were known, it could be used as a reference system for fluids with continuous intermolecular potentials. This approach has resulted in very successful perturbation theories for dense fluids^{4,5}.

In view of the important role that the hard sphere system has played, it is somewhat surprising that virtually no work has been done on the dynamics of non-spherical molecules with impulsive interactions. In fact, the work of Rebertus and Sando on the dynamics of hard spherocylinders is, to our knowledge, the only published MD study of "hard", non-spherical molecules⁶ (see, however, ref.7). Admittedly, the rough-sphere fluid has been studied in detail by MD⁸, but rough-spheres are not really typical for non-spherical molecules. There are however other "hard" systems which, in their simplicity, are comparable to the hard-sphere fluid. One such system, a fluid consisting of infinitely thin, hard rods of length L ("hard-lines") is the subject of the present letter. In this letter, we present the results of MD simulations on a

system of hard-lines, over a range of densities. We compare the results of these simulations with theoretical predictions for the density dependence of transport properties. Although we will briefly indicate the nature of these theoretical predictions, we must refer the reader to a subsequent publication⁹ for a more detailed discussion. Similarly, only certain features of the computational method that we used will be mentioned here; ref.9 will contain a detailed discussion.

The hard-line fluid is remarkable in that all of its structural properties are those of an ideal gas, whereas all of its transport properties are non-ideal, and strongly dependent on density. The absence of structural correlations is a direct consequence of the fact that the hard-line system has zero excluded-volume; at any density, any molecular position and orientation (but for a set of measure zero) is equally likely. Obviously, as the configurational part of the partition function equals $V^N/N!$, the pressure of a hard-line fluid must follow the ideal gas law and no thermodynamic phase transitions are possible in this system. In contrast, the dynamics of hard-lines is very sensitive to the presence of other lines. Theoretical predictions can be made about the dynamics of hard-lines (in particular about translational and rotational diffusion), using two very different approaches. The first is the well-known Enskog method for computing transport properties (we use the word "Enskog-theory" in the sense explained in refs.10 and 8). Due to the absence of structural correlations in the hard-line system, the following, very simple expressions result for the diffusion constant D , and the angular momentum correlation time τ_J ⁹:

$$D = 2.303 \dots / \rho^* \quad (1)$$

and

$$\tau_J = 1.705 \dots / \rho^* \quad (2)$$

In the above expressions, reduced units have been used: $\rho^* = \rho L^3$, where ρ is the number density and L the length of the line. We define L to be the unit of length, m (the mass of the line) to be the unit of mass, and kT to be the unit of energy. I , the moment of inertia of the rods, is chosen to be equal to $1/12$, which corresponds to a uniform mass distribution. Other choices for I are possible; they result in other numerical

constants in eqns.1-2 (and 3), below). The collision frequency in a hard-line fluid can be calculated exactly:

$$\Gamma = 1.23766 \dots \rho^* \quad (3)$$

Eq.3 is valid in the thermodynamic limit; the explicit N-dependence of Γ can be worked out⁹. It is important to note that eq.3 is exact; it provides our most important, non-trivial check on the MD results to be presented below.

At high densities eq.3 is still valid, but the Enskog expressions (eqns.1-2) may fail. However, it is precisely at high densities ($\rho^* \gg 1$) that theoretical predictions can be made about rotational and translational diffusion, using scaling arguments similar to those presented by Doi and Edwards¹¹ (henceforth referred to as DE). These authors have developed a theory of Brownian dynamics of rod-like macromolecules in concentrated solutions. One of the central predictions of the DE theory is that for thin, flexible rods the following relation should hold between the rotational diffusion constant D_r and the longitudinal translational diffusion constant D_l (i.e. along the rod axis):

$$D_r \sim D_l / \rho^{*2} \quad (4)$$

The basic idea behind this expression is that the reorientation of the rods is constrained by the presence of other rods. Only when one of the constraining rods diffuses away (typically, in a time $1/D_l$), can the constrained molecule perform an angular jump of order $\theta \approx \rho^{*-1}$. Several attempts have been made to test the DE theory experimentally^{12,13}, using light-scattering to study the rotational dynamics of long, rod-like viruses. There are however some discrepancies between theory and experiment, and it is not obvious at present whether these discrepancies are due to deficiencies of the DE theory or to the fact that real viruses are actually not completely rigid, nor infinitely thin. MD simulations on a hard-line system should provide a more direct test of the DE theory. It should be noted, however, that the DE theory was derived for rods performing Brownian motion in a viscous fluid. For smooth, hard-lines, eq.4 has to be modified slightly⁹, and reads:

$$D_{\perp} \sim 1/\rho^{*2} \quad (4a)$$

(The original eq.4 should hold for rough hard lines). The high-density behaviour of D_{\perp} can be predicted by extending the scaling arguments used by Doi and Edwards. One arrives at a remarkable prediction, namely that D_{\perp} should diverge at high densities:

$$\lim_{\rho^* \rightarrow \infty} D_{\perp} \sim \rho^{*1/2} \quad (5)$$

The reason for this unexpected behaviour is that, during a collision, only forces perpendicular to the molecular axis act on a smooth hard-line. As a simple approximation for the rate of change of the correlation function of the longitudinal velocity, $C_{\parallel}(t) \equiv \langle v_{\parallel}(0)v_{\parallel}(t) \rangle$, we may write:

$$C_{\parallel}(t) = -\gamma \langle \sin^2 \theta(t) \rangle C_{\parallel}(t) \quad (6)$$

where the "friction constant" γ is proportional to the collision frequency, $C_{\parallel}(t) \sim \exp(-\gamma \langle \omega^2 \rangle t^3/3)$, where $\langle \omega^2 \rangle$ is the mean square rotation frequency of the rods. In the rotational diffusion regime ($\Gamma^{-1} \ll t \ll D_{\perp}^{-1}$), $C_{\parallel}(t)$ decays as $\exp(-2\gamma D_{\perp} t^2)$, and for $t \gg D_{\perp}^{-1}$, it should decay as $\exp(-2/3 \gamma t)$. At high densities the correlation function should become predominantly Gaussian, and hence $D_{\perp} = (\pi/2\gamma D_{\perp})^{1/2} \sim \rho^{*1/2}$ (eq.5). Unlike D_{\parallel} , D_{\perp} should decrease with increasing ρ^* , but somewhat faster than predicted by eq.1:

$$\lim_{\rho^* \rightarrow \infty} (D_{\perp}/D_{\text{Enskog}}) = 2/3 \quad (7)$$

No anomalous behaviour is predicted for τ_J ; this, in itself, has interesting consequences because combination of eqns.2 and 4 yields:

$$\lim_{\rho \rightarrow \infty} \tau_J D_{\perp}^{-1} \sim \rho^* \quad (8)$$

which implies that the Hubbard relation ($\tau_J/D_{\perp} = \text{constant}$)¹⁴ fails at

high ρ^* .

The algorithm to solve the equations of motion for the hard-line fluid is rather different from most conventional MD procedures. To find the time t_c at which two moving, rotating lines (i and j) are due to collide, the program searches for the roots of the following equation:

$$F(t) \equiv \vec{r}_{ij}(t) \cdot \vec{u}_i(t) \wedge \vec{u}_j(t) = 0 \quad (9)$$

Here \vec{r}_{ij} is the distance between the centres of mass of rods i and j, \vec{u}_i (\vec{u}_j) is the orientation vector along the molecular axis. A necessary (but not sufficient) condition for a collision is: $F(t_c) = 0$, which implies that \vec{r}_{ij} , \vec{u}_i and \vec{u}_j are all in one plane. Next, one has to test whether the coplanar lines do actually intersect. If not, the program searches for the next zero of $F(t)$ and repeats the test. We took great care to ensure that no roots of $F(t)$, and hence no collisions, were overlooked. In practice, the routine that searches for the next collision is written in such a way that the number of computations of $F(t)$ (which are rather time-consuming) is kept to a minimum. More details about the program are given in ref.9. The collision dynamics is completely determined by the condition that energy, angular momentum and linear momentum are conserved, plus the assumption that the impulsive force between two colliding lines (\vec{f}_{ij}) is perpendicular to both lines (the condition of "smoothness"). This latter condition guarantees that smooth hard-lines obey the ideal gas-law; the virial vanishes identically, because $\vec{f}_{ij} \cdot \vec{r}_{ij} = 0$.

Several tests were performed to check whether the program was functioning properly. It was found that energy and momentum were conserved to better than 1 in 10^{10} , the average rotational and translational temperatures were equal (within the noise), the dynamics was reversible for at least 1000 collisions and, most importantly, the density dependence of the collision frequency was found to obey eq.3. Computing time was long, but not excessive: on a CYBER 170-750 computer, 20,000 collisions in a 500 particle system (with periodic boundary conditions), at a density of $\rho^* = 16$, took about 2800 CPU seconds. In a conventional MD simulation, a production run is preceded by an equilibration run. In hard-line simula-

tions, the equilibration step can be eliminated, provided that the initial molecular positions and orientations are carefully randomized, while the initial velocities and angular momenta are distributed according to the Maxwell-Boltzmann law.

Runs were done on a 100-particle system at densities $\rho^* = 1, 2, 4, 6$ and 8, and on a 500-particle system for $\rho^* = 16, 24, 32$ and 48. Compared to typical runs on a hard-sphere system, the runs were quite short (20,000 collisions). Consequently, we could only study single particle properties; the estimated noise in the computed correlation functions is 1-2%. (ACF's) of the molecular centre of mass velocity $\langle \vec{v}(\tau) \cdot \vec{v}(t+\tau) \rangle$ (decomposed into components parallel and perpendicular to the molecular orientation at time τ) were computed, as well as the ACF's of the molecular angular momentum ($C_{J_l}(t) \equiv \langle \vec{J}(0) \cdot \vec{J}(t) \rangle$). In addition, we computed the orientational correlation functions $\langle P_1(\vec{u}(0) \cdot \vec{u}(t)) \rangle \equiv C_1(t)$ and $\langle P_2(\vec{u}(0) \cdot \vec{u}(t)) \rangle \equiv C_2(t)$, where $\vec{u}(t)$ is the molecular orientation at time t and $P_1(P_2)$ the 1st (2nd) Legendre polynomial. All correlations were studied out to 25 collision times.

At low densities ($\rho^* < 8$), the velocity and angular momentum ACF's decay exponentially with a slope that agrees well with the Enskog predictions. At these densities, the orientational correlation functions $C_1(t)$ and $C_2(t)$ closely follow the behaviour predicted by the J-diffusion model (with a "collision frequency" equal to $1/\tau_J$ Enskog)^{14,16,9}. At high densities, all correlation functions show marked deviations from the Enskog (c.q. J-diffusion) predictions. With increasing density, the decay of $C_{J_l}(t)$ and $\langle v_{\perp}(0) v_{\perp}(t) \rangle$ becomes faster than exponential, and for $\rho^* > 30$ both ACF's develop a negative minimum after about 5 collision times. $C_1(t)$ and $C_2(t)$ decay exponentially at high ρ^* ; from the slopes of these exponential correlation functions we determined the effective rotational diffusion constant D_r , using the relation:

$$\frac{d}{dt} \ln C_l(t) = - l(l+1)D_r \quad (l = 1, 2). \quad (10)$$

Fig.1 shows a plot of D_r^{-1} vs. ρ^{*2} . Clearly, at densities $\rho^* > 8$, the (modified) Doi-Edwards prediction (eq.4a) is in good agreement with the

observed density dependence of D_r . Fig.2 shows the time dependence of $\log \langle v_{\perp}(0)v_{\perp}(t) \rangle (\equiv \log(C_{\perp}(t)))$. Several points should be noted. First of all, the initial slope of $\log(C_{\perp}(t))$ (out to ~ 2 collision times) is very flat; in fact, it follows the predicted t^3 -dependence. One should also note the dramatic positive departures from the Enskog predictions; for $\rho^* > 24$, v_{\perp} persist much longer than 25 collision times. The criteria formulated below eq.6 predict predominantly Gaussian behaviour of $C_{\perp}(t)$ for $\Gamma^{-1} \ll t \ll D_r^{-1}$. For densities $\rho^* = 32$ and 48 , $D_r^{-1} > 25$ collision times. At these densities one might therefore hope to observe Gaussian decay of $C_{\perp}(t)$ in fig.2. Inspection of fig.2 suggests that the decay of $C_{\perp}(t)$ is, in fact, simply exponential. But when $\log(C_{\perp}(t))$ is plotted vs. t^2 , it is found that the high density data fit equally well to a Gaussian. On basis of the present results we are unable to eliminate either possibility. The diffusion coefficients D_{\perp} and D_{\parallel} were obtained from the integrals of the transverse and longitudinal velocity ACF's. In order to perform the integrals of $C_{\perp}(t)$, for $\rho > 24$, we had to extrapolate $C_{\perp}(t)$ for times longer than 25 collision times. Both Gaussian and exponential extrapolations were used. It is seen in fig.3 that, irrespective of the nature of the extrapolation, D_{\perp} increases with increasing ρ^* for $\rho^* > 24$. The corresponding Enskog predictions are shown for the sake of comparison. The results shown in fig.3 strongly suggest that D_{\perp} diverges as $\rho^* \rightarrow \infty$. On basis of the present data we are, however, unable to confirm or reject the $\rho^{*1/2}$ -dependence predicted by eq.5. Table I contains a summary of the transport properties obtained from the MD simulations. Tabulated are: the collision frequency (Γ), the diffusion constants D_{\perp} and D_{\parallel} , the decay time of $C_{\perp}(t)$ (τ_{\perp}) and the orientational correlation times τ_1 and τ_2 .

Table I: Density dependence of computed collision frequency (Γ), longitudinal and transverse diffusion constants (D_{\parallel} and D_{\perp}), and the decay times of the correlation functions of angular momentum (τ_J), $C_1(t)$ (τ_1) and $C_2(t)$ (τ_2).

ρ^*	Γ	D_{\parallel}	D_{\perp}	τ_J	τ_1	τ_2
1	1.24	2.59	2.30	1.69	0.12	0.49
2	2.44	1.37	1.05	0.93	0.14	0.30
4	4.89	0.82	0.51	0.44	0.21	0.22
6	7.24	0.60	0.36	0.31	0.25	0.17
8	9.99	0.53	0.25	0.20	0.30	0.18
16	19.8	0.50	0.11	0.088	0.51	0.23
24	30.2	0.49	0.073	0.058	0.73	0.36
32	40.0	0.50	0.049	0.039	0.93	0.36
48	61.5	0.76	0.021	0.021	1.54	0.56

References

- ¹ J.P. Hansen and I.R. McDonald, *Theory of Simple Liquids*, A.P., London, 1976.
- ² B.J. Alder, D.M. Gass and T.E. Wainwright, *J. Chem. Phys.* 53, 3813 (1970).
- ³ J.J. Erpenbeck and W.W. Wood in: *Statistical Mechanics B, Modern Theoretical Chemistry*, Vol.6, B.J. Berne ed., Plenum, N.Y. (1977).
- ⁴ J.A. Barker and D. Henderson, *J. Chem. Phys.* 47, 4714 (1967).
- ⁵ J.D. Weeks, D. Chandler and H.C. Andersen, *J. Chem. Phys.* 54, 5237 (1971).
- ⁶ D.W. Rabertus and K.M. Sando, *J. Chem. Phys.* 67, 2585 (1977).
- ⁷ A. Bellemans, J. Orban and D. van Belle, *Mol. Phys.* 39, 781 (1980).
- ⁸ J. O'Dell and B.J. Berne, *J. Chem. Phys.* 63, 2376 (1975), B.J. Berne, id.66, 2821 (1977), C.S. Pangali and B.J. Berne, id.67, 4571 (1977).
- ⁹ D. Frenkel and J.F. Maguire, to be published.
- ¹⁰ D. Chandler, *J. Chem. Phys.* 60, 3500 (1974).

- 11 M. Doi, J. Phys. (Paris) 36, 607 (1975), M. Doi and S.F. Edwards, J. Chem. Soc. Faraday. Trans.II, 74, 560 (1978).
- 12 J.F. Maguire, J.P. McTague and F. Rondelez, Phys. Rev. Lett. 45, 1891 (1980).
- 13 J.F. Maguire, J. Chem. Soc. Faraday. Trans.II, 77, 513 (1981).
- 14 P.S. Hubbard, Phys. Rev. 131, 1155 (1963).
- 15 D. Chandler, J. Chem. Phys. 60, 3508 (1974).
- 16 W.A. Steele, Adv. Chem. Phys. XXXIV, 1 (1976).

Figure Captions

- Fig.1 Inverse rotational diffusion constant (D_r^{-1}) vs. the square of the reduced density (ρ^{*2}). D_r was obtained using eq.7 on $C_1(t)$ (O) and on $C_2(t)$ (*). The dashed line is a best fit to the high density points.
- Fig.2 $\log C_1(t)$ vs. t . t is expressed in mean collision times.
 (*): $\rho^* = 1$, (●): $\rho^* = 8$, (∇): $\rho^* = 16$, (▼): $\rho^* = 24$, (O): $\rho^* = 32$,
 (▲): $\rho^* = 48$.
- Fig.3 D_{\perp} (●), D_{\parallel} (■) and $\text{Tr } D = (2D_{\perp} + D_{\parallel})/3$ (*) vs. reduced density. For $\rho^* = 32$ and 48, 2 values for D_{\perp} are shown; the lower value is based on a Gaussian extrapolation, the higher one on an exponential extrapolation (see text). The solid curve is the Enskog prediction (eq.1).

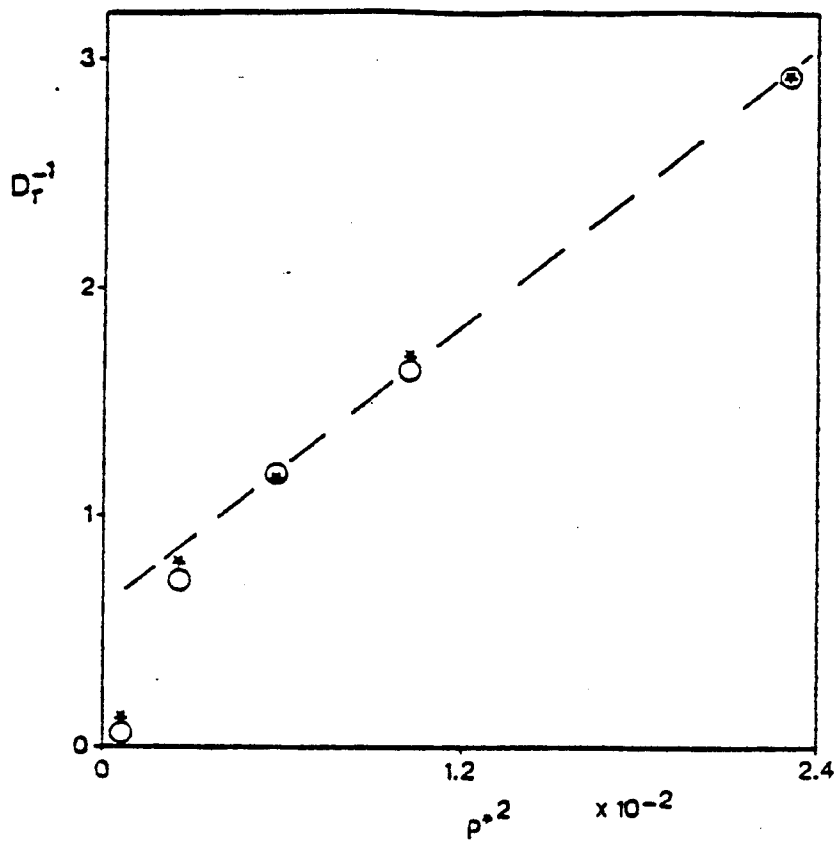


Fig.1

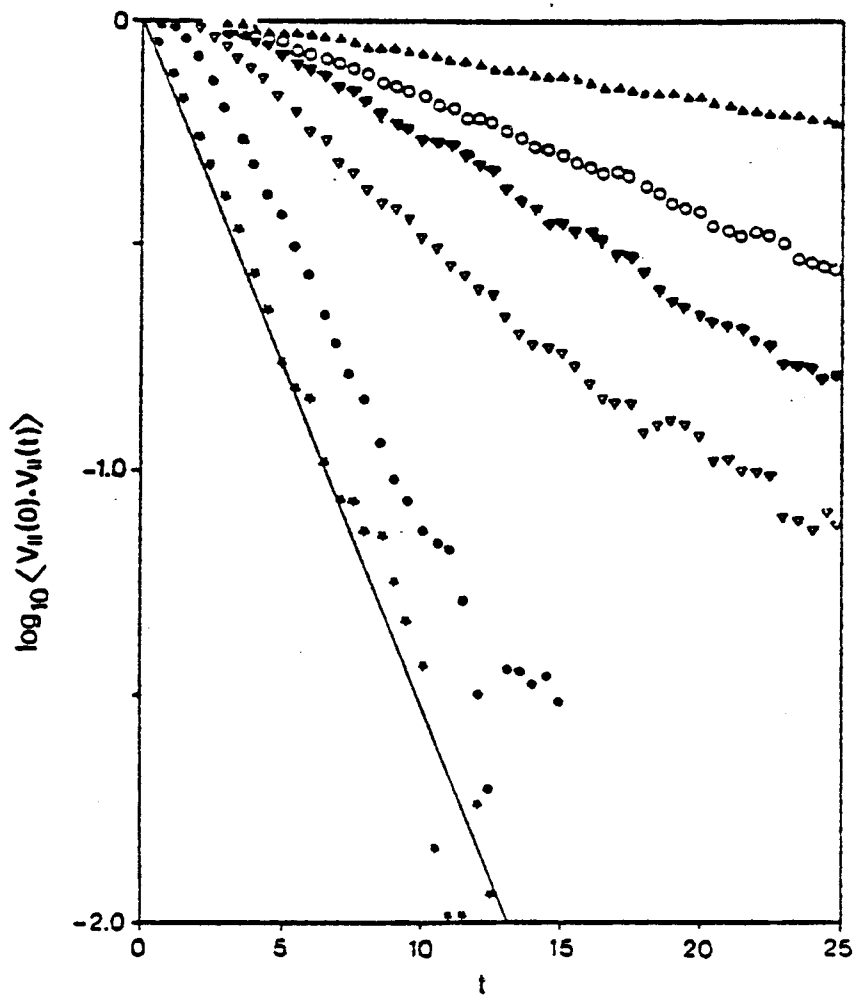


Fig.2

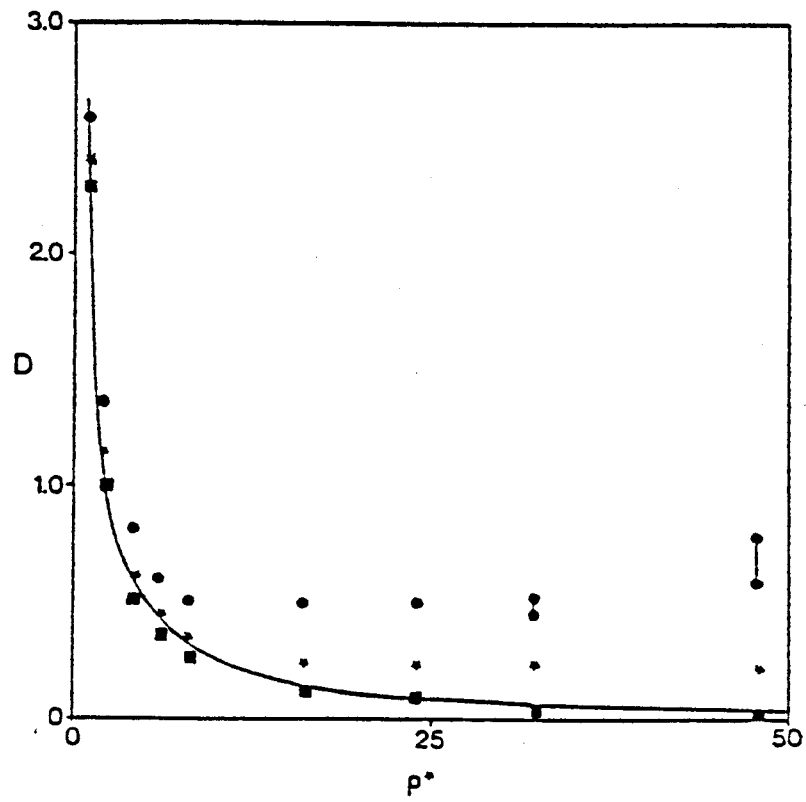


Fig.3